Integration of sensory and motor representations of single fingers in the human cerebellum

Tobias Wiestler, David J. McGonigle and Jörn Diedrichsen

J Neurophysiol 105:3042-3053, 2011. First published 6 April 2011; doi:10.1152/jn.00106.2011

J Neurophysiol 105: 3042–3053, 2011.
First published April 6, 2011; doi:10.1152/jn.00106.2011.

Integration of sensory and motor representations of single fingers in the human cerebellum

Tobias Wiestler,[1,2] David J. McGonigle,[3,4] and Jörn Diedrichsen[1,2]

[1]*Institute of Cognitive Neuroscience, University College London, London;* [2]*Wolfson Centre for Cognitive and Clinical Neuroscience, School of Psychology, Bangor University, Gwynedd; and* [3]*Cardiff University Brain Research and Imaging Centre, School of Psychology, and* [4]*School of Bioscience, Cardiff University, Cardiff, United Kingdom*

Submitted 11 February 2011; accepted in final form 3 April 2011

Wiestler T, McGonigle DJ, Diedrichsen J. Integration of sensory and motor representations of single fingers in the human cerebellum. *J Neurophysiol* 105: 3042–3053, 2011. First published April 6, 2011; doi:10.1152/jn.00106.2011.—The cerebellum is thought to play a key role in the integration of sensory and motor events. Little is known, however, about how sensory and motor maps in the cerebellum superimpose. In the present study we investigated the relationship between these two maps for the representation of single fingers. Participants made isometric key presses with individual fingers or received vibratory tactile stimulation to the fingertips while undergoing high-resolution functional magnetic resonance imaging (fMRI). Using multivariate analysis, we have demonstrated that the ipsilateral lobule V and VIII show patterns of activity that encode, within the same region, both which finger pressed and which finger was stimulated. The individual finger-specific activation patches are smaller than 3 mm and only show a weak somatotopic organization. To study the superposition of sensory and motor maps, we correlated the finger-specific patterns across the two conditions. In the neocortex, sensory stimulation of one digit led to activation of the same patches as force production by the same digit; in the cerebellum, these activation patches were organized in an uncorrelated manner. This suggests that, in the cerebellum, a movement of a particular finger is paired with a range of possible sensory outcomes. In summary, our results indicate a small and fractured representation of single digits in the cerebellum and suggest a fundamental difference in how the cerebellum and the neocortex integrate sensory and motor events.

functional magnetic resonance imaging; multivoxel pattern analysis; motor cortex; sensory cortex

THE CEREBELLUM IS THOUGHT to play an important role in sensorymotor integration (Bastian 2006; Wolpert et al. 1998). In this study we have used functional magnetic resonance imaging (fMRI) to study in detail the sensory and motor representations of individual fingers in the human cerebellum. Previous studies have shown that both the anterior and posterior motor regions of the human cerebellum are activated during hand movements (Grodd et al. 2001; Rijntjes et al. 1999). The same regions are also activated, albeit to a much lesser degree, during noxious stimulation (Casey et al. 1996), passive finger movements (Mima et al. 1999; Thickbroom et al. 2003), and vibrotactile stimulation (Fox et al. 1985; Tempel and Perlmutter 1992). All these studies, however, have left open the question whether the cerebellum contains a representation of individual finger movements comparable to those in primary sensory and motor cortex (Indovina and Sanes 2001; Kaas et al. 1979; Merzenich et al. 1987; Sur et al. 1982; Woolsey et al. 1979). If the human cerebellum indeed contains such a map, we should be able to detect different activity patterns for different fingers and to determine how sensory and motor maps superimpose.

Because of the limits on spatial resolution of fMRI, the detection of small and potentially unordered representations constitutes a challenge. In the primary somatosensory cortex (S1), digit representations are arranged in an orderly sequence of patches with a diameter of 4–5 mm and thus can be detected by comparing the activations maps for each finger (Sanchez-Panchuelo et al. 2010). In the cerebellar cortex, however, such finger representations may be smaller and less well organized. For example, based on data from the rat whisker system in Crus I, some authors have argued that the cerebellar sensory representations are small and fractured (Bower and Woolston 1983). Others have argued for a more systematic organization. For example, stimulation of the forepaw of cats activates an ordered sequence of parasaggital cerebellar microzones, groups of Purkinje cells with the same climbing fiber input (Apps and Garwicz 2005). These microzones also receive matched mossy fiber input (Pereira et al. 2009). There is, however, general agreement that such representations are smaller than those found in the cerebral cortex.

It should be stressed at this point that although our knowledge of the origin of the cerebellar blood oxygen level-dependent (BOLD) signal is still limited, recent evidence indicates that mossy fiber and parallel fiber signaling is the main determinant of activity-induced BOLD changes (Attwell and Iadecola 2002; Diedrichsen et al. 2010; Zhang et al. 2003). Thus BOLD signal from the cerebellar cortex most likely reflects the spatial patterns of sensory and motor input to the granule cell system.

Given the small spatial scale of digit representations, how can we best detect them using fMRI? Although the cerebellum may lack an orderly map of individual digits, groups of microzones that respond preferentially to a particular finger are likely clustered together in space. We refer to such groups as "digit patches" and stress, first, that there may be multiple patches for the same digit within a region; second, that these may overlap with patches for other digits; and third, that they may be arranged without any somatotopic gradient. Because the spatial arrangement of such digit patches is likely to differ across individuals, they cannot be detected using traditional univariate analysis. Such analysis would require the existence of areas in which there are systematic activation differences between fingers across participants, e.g., a region where, rela-

Address for reprint requests and other correspondence: T. Wiestler, Institute of Cognitive Neuroscience, Univ. College London, Alexandra House, 17 Queen Square, London WC1N 3AR, United Kingdom (e-mail: Tobias.Wiestler.09@ucl.ac.uk).

tive to other fingers, thumb movement always leads to more activation.

In contrast, local multivariate pattern analysis (Kriegeskorte et al. 2006) can be used to identify regions in which participants show significantly different finger-related patterns, even if these do not superimpose in a finger-by-finger fashion in a group analysis. Furthermore, multivariate analysis can also identify regions in which these finger-specific patterns consist of local signal increases and decreases, without changing the activation level of the region overall (Fig. 1A).

Therefore, this method relates more closely to the criterion employed in neurophysiology, where a region is considered to be involved in a task if its neurons modulate (i.e., either increase or decrease) their firing rates in relation to an experimental variable, even if the average activity in the region does not change and if the spatial distribution of these modulations differs across individual brains. Multivariate analysis has been successfully employed in the visual system to study neural representations that are small and do not systematically align across individuals (Cox and Savoy 2003; Haxby et al. 2001; Haynes and Rees 2005a; Kamitani and Tong 2006; Kriegeskorte et al. 2008b; Swisher et al. 2010); however, this is the first application of this technique in the cerebellum.

We used an event-related design (Fig. 1*B*) with a stimulation and a motor condition. In designing the tasks, we attempted to minimize the risk of movement in the stimulation condition and the contribution of sensory information in the motor condition. We therefore asked participants to produce repeated isometric presses with one finger (Fig. 1*B*) against a key equipped with a force sensor. Thus the main residual sensory information in the motor condition would be the stimulation of Golgi tendon organs and Merkel receptors. In the stimulation condition, we delivered a 100-Hz vibrotactile stimulus to the glabrous skin of a single fingertip, thereby activating mostly Meissner and Pacinian receptors (Johnson 2001) and minimizing the risk of overt movement.

Using multivariate analysis, we were able to reveal overlapping sensory and motor representations of single digits in two ipsilateral regions, one in lobule V and one in lobule VIII. We then studied the characteristics of these digit representations in detail. First, we compared the results of the multivariate analysis with traditional mass-univariate approaches, showing a part-dissociation between finger-specific modulation of activation patterns and the overall size of the activation. We then asked our main question of how sensory and motor maps superimpose. Finally, we have described the size of the digit patches in the cerebellum and test for possible somatotopic gradients. In all these analyses, we compared the characteristics of the cerebellar digit representations to those found in S1 and M1. Our results suggest a fundamental difference in the representation of digits in the human neocortex and the cerebellum, with important implications on how these regions relate sensory and motor information.

METHODS

Participants. Two female and five male neurologically healthy volunteers participated in the study. All participants were right-handed, and their ages ranged from 20 to 22 yr. The ethics committee of the School of Psychology, Bangor University, approved all experimental procedures. The cortical data of these participants were used

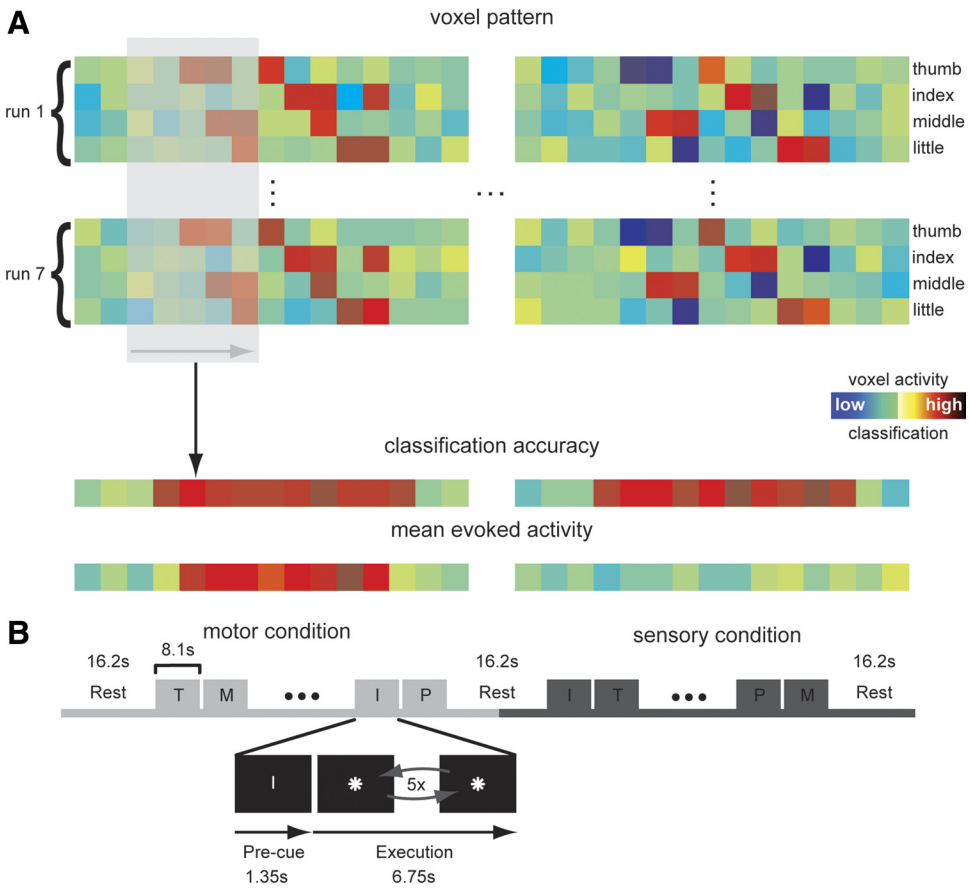

Fig. 1. Experimental methods. *A*: detecting finger representations using multivariate analysis. Each row indicates the activation pattern induced by finger presses or sensory stimulation in 2 hypothetical neural regions. In each region, there is a finger-specific blood oxygen level-dependent (BOLD) pattern that is replicable across multiple imaging runs. The searchlight (shaded box) method picks continuous groups of voxels and detects the presence of a local informative voxel pattern (classification accuracy). The region at *left* has only finger-specific BOLD increases and therefore shows increased activity when all fingers are compared against rest; the region at *right* shows both signal increases and decreases, which cancel each other out such that there is no overall evoked activity. Multivariate analysis can detect the finger-specific modulation of neural activity in both cases. *B*: in the motor condition, participants pressed keys with the finger indicated by the precue (T, thumb; I, index finger; M, middle finger; and P, little finger) 5 times, paced by an asterisk. In the sensory condition, a vibratory stimulus of 100 Hz was applied 5 times to the indicated fingertip. In each imaging run, both conditions were performed in counterbalanced order separated by short rest phases.

as example data in a method article describing the surface-based searchlight technique (Oosterhof et al. 2010), and both cortical and cerebellar data were used in a technical note on the decomposition method (Diedrichsen et al. 2011).

Apparatus. To stimulate individual fingertips and to record individual finger forces, we developed an fMRI-compatible device with five piano-style keys. Each key had a small groove into which the fingertip could be placed. Within the groove was a hole through which a small pin (1-mm radius) could be vibrated with finely controlled frequency and amplitude using a piezo motor. The forces applied to the keys were recorded via quantum tunneling composite pills (ref. N18BU; Maplin Electronics, Rotherham, UK). The stimulation box was controlled from outside the scanning room, with a filter panel preventing leakage of radio frequency (RF) noise into the MR environment. The visual instructions and feedback were projected from outside the scanner room onto a back-projection screen, which was viewed by the participants through a mirror.

Scan acquisition. The imaging data were acquired on a Phillips Achieva 3T scanner (Philips, Best, The Netherlands). For the functional scans, we used an echo planar imaging sequence (EPI) with a voxel size of $1.8 \times 1.8 \times 2$ mm^3. Data acquisition for the cerebellum and the cerebral cortex took place in two separate sessions. Each region was covered with 38 axial slices (no gaps; TR = 2.7s), using sensitivity encoding with a factor of 2 (Pruessmann et al. 1999). Runs started with 6 dummy scans and consisted of 128 data images. The T1-weighted structural images were acquired with a volumetric magnetization-prepared rapid gradient echo (MPRAGE) sequence using a voxel size of $1 \times 1 \times 1$ mm^3.

Procedure. Before the scan acquisition, all participants underwent a training session of four runs in which they were familiarized with the task. They then participated in two counterbalanced scanning sessions (1 for the cortex, 1 for the cerebellum), separated by at least 12 h. Each scanning session comprised 7 runs, each of which consisted of 16 force trials and 16 stimulation trials, separated by a pause of 16.2 s (Fig. 1*B*). The sequence of conditions was counterbalanced across runs and participants. A single trial lasted 8.1 s, and within each condition, every finger was repeated four times in randomized order. To obtain enough repetitions for each finger, we used only *digits 1*, *2*, *3*, and *5* of the right hand and excluded the ring finger from the experiment. Each trial started with a red letter on the screen to indicate the digit to be pressed or stimulated. During the motor condition, participants made five isometric key presses with the indicated finger. Presses were paced by the appearance of a white asterisk on the screen every 1.35 s and required a force >1 N to be registered. The asterisk turned green if participants pressed the correct finger and red otherwise. In the stimulation condition, we applied a vibratory stimulus every 1.35 s for 0.94 s, five times to a single fingertip. The stimulation frequency was 100 Hz, with small pauses of 20 ms inserted every 110 ms to reduce the possibility of central or peripheral habituation. As in the motor condition, a white asterisk was presented as a visual pacing signal. The onset of the vibratory stimuli was jittered within an interval of −200 to +200 ms around the presentation of the asterisk to reduce habituation. The stimulation intensity was individually adjusted so that the subjective stimulation intensity was comparable across fingers.

Imaging data analysis. We analyzed the functional imaging data using SPM5 (http://www.fil.ion.ucl.ac.uk/spm/) (Friston et al. 1993) and custom-written routines in MATLAB (The MathWorks, Natick, MA). We first realigned the slices in time to correct for the ascending order of slice acquisition. The images were spatially realigned to the first functional image of the session using a six-parameter rigid-body transformation. To remove slowly varying trends, we high-pass filtered the data with a cutoff frequency of 1/128 s. The spatially unsmoothed data were fitted using a linear model with regressors that represented the four trials of each finger (separately for motor and stimulation conditions) within each run. These regressors were boxcar functions (length 8.1 s), convolved with the standard hemodynamic response function. The resultant beta estimates (regression coefficients) indicate how much each voxel changed its activation for each run, condition, and finger and were used as data for the multivariate analysis. The functional images were coregistered to the individual anatomic images (Collignon et al. 1995). Because we wanted to distinguish between functional data from the primary motor and sensory cortices, special care was taken that the alignment was exact at the central sulcus, and hand correction was applied as necessary.

For the group analysis, we applied three different methods of intersubject alignment. First, the cortical data were normalized by aligning the individual anatomic images to the Montreal Neurological Institute (MNI) template with a nonlinear segmentation and normalization algorithm (Ashburner and Friston 2005). Second, the cortical surface of left hemisphere of each subject was reconstructed, inflated to a spherical representation, and finally aligned to an average surface-based atlas using the program Freesurfer (Dale et al. 1999). This normalization ensured a good overlap of the fundus of the central sulcus across participants. Third, for the cerebellar data, we isolated the cerebellum from the rest of the brain and aligned the data to a high-resolution cerebellum-only template (SUIT) (Diedrichsen 2006).

Classification. To detect digit representations in the cerebellum and neocortex, we selected a group of spatially contiguous voxels and tested for each participant individually and separately for the motor and stimulation conditions whether the activity patterns across these voxels differed significantly between digits. This was achieved using a linear classifier (Haxby et al. 2001; Haynes and Rees 2005a; Misaki et al. 2010).

Inputs to the classifier were the 4×7 pattern vectors x_i, the beta estimates for a set of N voxels for each finger and run. We trained the classifier using 24 pattern vectors from 6 runs. From these training data, we estimated the overall $N \times N$ voxel-covariance matrix Σ and the $N \times 1$ mean vectors of the four classes (fingers) μ_c. Because Σ was ill-conditioned, we regularized the covariance estimate by adding a small constant (1% of the mean of the diagonal elements) to the diagonal. This regularization makes the covariance matrix invertible while still retaining the advantage that noisy or highly correlated voxels are downweighted (Pereira et al. 2009).

The discriminant function for each class (g_c) is, up to a constant, the log-likelihood that the pattern x belongs to class c:

$$g_c(x) = \mu_c^T \Sigma^{-1} x - \frac{1}{2} \mu_c^T \Sigma^{-1}. \quad (1)$$

As test patterns, we used the four remaining digit patterns of the 7th run. We assigned the test pattern x to the class c with the maximum likelihood:

$$\hat{c} = \arg_c \max\left[g_c(x)\right]. \quad (2)$$

By retraining and cross-validating over all possible test and training sets, we determined the average cross-validation accuracy each set of voxels. All classification accuracies reported in this article are based on this cross-validation approach, thereby providing a statistically unbiased measure of how much information a voxel neighborhood (see below) contains about which finger moved or was stimulated.

Volume-based searchlight. For the identification of digit representations in the cerebellar cortex, we utilized a volume-based searchlight approach (Kriegeskorte et al. 2006). The data for the classification came from a 6-mm sphere around a chosen center voxel, which included ~145 voxels. We restricted all calculations to cerebellar voxels using an automatic masking algorithm provided by the SUIT toolbox (Diedrichsen 2006). We calculated the classification accuracy for each group of voxels and assigned it to the center voxel of the sphere. By moving the sphere through the whole volume, we generated an accuracy map. Voxels that had less than 10 voxels as a neighborhood were excluded from the analysis.

Surface-based searchlight. The two main regions for digit representation in the cerebral cortex are the primary motor and somatosen-

sory cortices. Whereas anatomically these regions are clearly separated by the central sulcus, they abut one another in volume. A volume-based searchlight, as employed for the cerebellum, would therefore combine voxels from both sensory and motor cortices into a single classifier. To measure the information content of these regions separately, we used a surface-based searchlight method (Oosterhof et al. 2010). We started with a representation of the pial surface and the gray matter-white matter boundary, which were generated by the program Freesurfer (Dale et al. 1999). For each surface node, we then determined all nodes within a certain radius, with the distance measured along the intermediate surface (Peyre 2008). The classification was then based on voxels that enclosed on of the selected nodes, either from the white or pial surface. For each center node, we adjusted the radius such that each searchlight contained 145 voxels. We then assigned the cross-validation accuracy of the classifier as a measure of information to the center node. By moving the center node across the surface, we built up a surface map of classification accuracies.

Regions of interest. To compare the organization of digit representations across different regions, we utilized an anatomically defined region-of-interest approach. We focused our analysis on four regions that revealed significant digit representations: the left primary somatosensory and motor cortices and the right lobules V and VIII of the cerebellum. The cortical regions were defined on a surface representation, guided by anatomic cytoarchitectonic evidence (Geyer et al. 2001). For the primary motor cortex, we selected the region between the fundus of the central sulcus and the crest of the precentral gyrus, encompassing approximately Brodmann area 4. For the primary somatosensory cortex, we selected the region between the fundus of the central sulcus to the crest of the postcentral gyrus, encompassing Brodmann area 3b and parts of 3a and 1. Both regions were defined on the surface representation along the whole length of the central sulcus. As for the surface-based searchlight, we then selected all voxels that included any node of the region either on the pial or white matter surface. Despite this surface-based definition, there was still a single layer of voxels in the middle of the central sulcus that was included in both regions. To minimize the overlap, we therefore excluded these voxels from both the S1 and M1 regions of interest.

The cerebellar regions were defined based on a probabilistic atlas of the cerebellum (Diedrichsen et al. 2009). Because we were only interested in functional signal from gray matter, we only included voxels that were assigned a probability of ≥ 0.1 of being gray matter in the probabilistic tissue segmentation (Ashburner and Friston 2005). This relatively low threshold ensured that all voxels that partially consisted of gray matter were included while rejecting voxels that were clearly situated in white matter.

Representational similarity-pattern component model. To assess the superposition of the sensory and motor maps, we calculated the correlations between stimulation and motor pattern (Haynes and Rees 2005b; Kriegeskorte et al. 2008a; Mur et al. 2009; Norman et al. 2006). We compared the average correlations between the stimulation and motor pattern for the same digit with the correlation for different digits.

When comparing correlations, or differences of correlations, across different regions, it is important to account for other factors that can influence these coefficients: For example, regions with high levels of fMRI noise will generally show lower correlations and lower differences of correlation. Alternatively, strong activation common to all conditions may increase correlations artificially. To account for these factors, we utilized a newly developed method that decomposes patterns into different components (Diedrichsen et al. 2011). The 56 measured patterns ($y_{i,j,k}$, ith condition $\times$ jth digits $\times$ kth run) were modeled as the sum of a component that was common to all digits within each condition (c_i), a component that was unique to the finger in each condition ($f_{i,j}$), noise components shared by all trials in a run ($r_{i,k}$) , and an independent noise component ($\varepsilon_{i,j,k}$):

$$y_{i,j,k} = c_i + f_{i,j} + r_{i,k} + \varepsilon_{i,j,k}. \quad (3)$$

The variance and covariance of these components across voxels was then estimated from the data. The finger components $f_{i,j}$ capture the patterns unique to force production or stimulation of each digit. We estimated the variance for the stimulation, $\sigma^2_{f_1}$, and for the motor condition, $\sigma^2_{f_2}$, and the covariance of patterns across the two conditions for the same digit, cov $(f_{1,j}, f_{2,j}) = \gamma_f$. Because the nonspecific determinants of the correlations are captured in the pattern component for the condition, noise, and run, the corrected correlation coefficient $\gamma_f/(\sigma_{f,1}, \sigma_{f,2})$ can serve as a direct measure of the similarity of finger patterns, normalized by the strength of the finger patterns in this region.

Using Monte Carlo simulations, we ensured that these estimates, in contrast to the sample correlations, were not influenced by changes in noise level, number of informative voxels, or spatial size of digit patches (Diedrichsen et al. 2011). Thus the new method allowed us to compare, across different anatomic regions, how similar the pattern evoked by isometric presses with a digit was to the pattern evoked by stimulating the same digit.

Spatial correlations. To compare the size of finger patches quantitatively across regions, we used the estimates of the pattern components (*Eq. 3*) to calculate the spatial covariance between each pair of voxels within a region. For example, for the finger component, the covariance estimate between voxel n and voxel m is

$$\mathrm{cov}_f(n, m) = \frac{1}{4}\sum_{i=1}^{4}\left(f^n_{i,j} - \bar{f}_{i,j}\right)\left(f^m_{i,j} - \bar{f}_{i,j}\right). \quad (4)$$

We then averaged the covariance across voxel pairs depending on their spatial distance. We used bins from 0.1 to 2.5 mm (directly neighboring) or 2.5 to 3.6 mm (diagonally neighboring), up to a total distance of 23.8 mm. We normalized the covariance by the variance to obtain a spatial autocorrelation function.

The smoothness of the underlying pattern component can be expressed using the full-width half-maximum (FWHM) of the spatial convolution kernel, which when used to smooth spatially independent data would result in the best fitting spatial autocorrelation function (Diedrichsen et al. 2011). Again, Monte Carlo studies were conducted so that the width of the spatial kernel could be estimated with relatively high accuracy, independent of the level of noise.

Somatotopy. Within the digit-related area of each anatomically defined region of interest, we searched for a somatotopic organization. As for the other analyses, we defined the digit-related area by selecting the voxels with the 20% highest classification accuracy in the region, and from these we selected the biggest spatially contiguous cluster. For each condition, we assigned a weight to every voxel i for every finger condition j using a softmax function across all fingers:

$$w_{i,j} = \frac{\exp(k\beta_{i,j})}{\sum_{m=1}^{4}\exp(k\beta_{i,m})} \quad (5)$$

In the extreme case, ($k >> 0$), the function would assign a value of 1 to the finger for which the voxel was most highly activated and a value of 0 to all other fingers. Considering the likely overlap of different digit patches, k was set to 0.8, resulting in a softer assignment. Similar results were obtained for a range of k from 0.6 to 1. The center of gravity (CoG) for each finger was calculated as the mean coordinate of all voxels weighted by $w_{i,j}$. To be able to compare locations across participants, we transformed the individual voxel coordinates to a standard atlas space: SUIT (Diedrichsen 2006) for the cerebellar regions and MNI152 for the cerebral regions.

RESULTS

Finger representations in the human cerebellum. We expected relatively small, and possibly unordered, sensory and

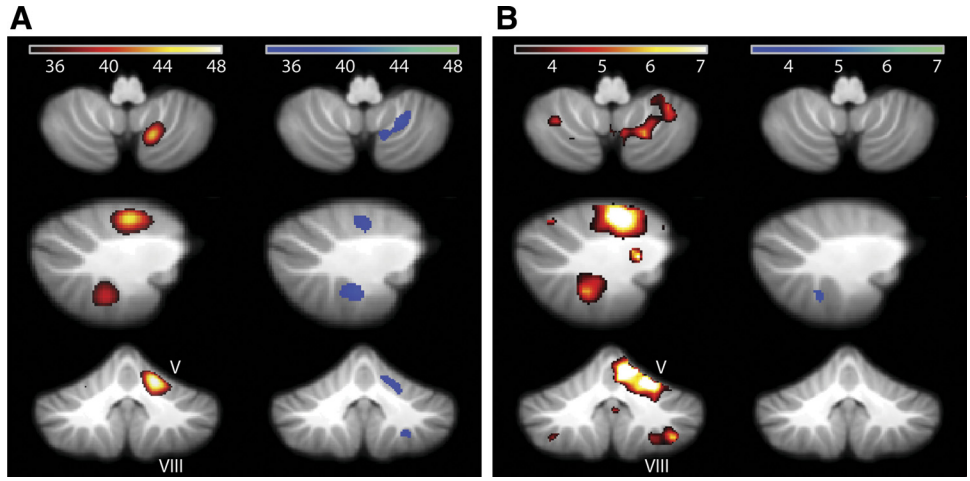

Fig. 2. Digit representations in the human cerebellum. Two digit representations in the human cerebellum are shown, revealed using local multivariate pattern analysis. *A*: multivariate analysis shows 2 regions (lobule V and VIII) that contain information about individual fingers in the motor (red) and stimulation (blue) conditions. The group-average maps show the cross-validated classification accuracy (threshold 34%, chance 25%). *B*: traditional mass-univariate analysis shows strong responses in the motor (red), but not in the stimulation (blue), condition. Group *t*-maps of the evoked BOLD signal for task vs. rest in motor (red) and stimulation (blue) conditions are shown at an uncorrected threshold of $t(6) = 3.14$, $P = 0.01$. The results are presented on axial ($z = -49$), parasaggital ($x = 21$), and coronal ($y = -52$) slices of the SUIT template (Diedrichsen 2006).

motor representations in the cerebellar cortex. To detect such representations, we used multivariate analysis to obtain a digit information map. This map showed whether the activity patterns evoked by different digits differed systematically from each other and therefore revealed whether the region encoded for (or contained information about) the pressed or stimulated finger.

In the cerebellum, the resulting maps of cross-validation accuracy showed two areas with above-chance accuracy in the ipsilateral, right hemisphere for both motor and stimulation conditions (Fig. 2*A*). These clusters were located in lobule V and lobule VIII and were significant in a random-effects group analysis, corrected for multiple tests (Table 1).

We also found a region in right Crus I that crossed the threshold of statistical significance in the stimulation condition (Table 1). However, the same region was not present in the motor condition. Although it is possible that there exists a third region for tactile processes, we did not consider this region further, because our main aim was to investigate the relationship between sensory and motor maps. In summary, our results show the existence of at least two overlapping motor and sensory representations of individual digits in the cerebellar cortex.

Finger representations in the human neocortex. We conducted a similar analysis for the neocortical data. We found an extended area with high classification accuracy along the central sulcus (Fig. 3, *A* and *B*). The main part of both sensory and motor representation is located in S1, encompassing a substantial portion of the postcentral gyrus. We also saw a digit representation in M1, with the best classification accuracies located at the bend of the precentral gyrus, the so-called hand knob (Yousry et al. 1997).

We localized neocortical digit representations using a surface-based searchlight (see METHODS). This technique minimizes the mixing of voxels from different sides of the central sulcus within a single classifier (Oosterhof et al. 2010). Therefore, we could map the informative regions in M1 and S1 fairly independently.

Evoked activity vs. information content. To compare the cortical and cerebellar digit representations quantitatively, we defined regions of interest for cerebellar lobules V and VIII, M1, and S1 based on anatomic criteria (see METHODS) for each participant. Within these regions, we then identified the digit representation for each condition by selecting the 20% of voxels with the highest accuracies in each region. The information content (assessed by average classification accuracy) for these voxels was substantially higher in the neocortical compared with the cerebellar regions (Fig. 4*A*). The classification accuracy in S1 was slightly higher for the sensory than for the motor condition. In contrast, the motor condition yielded slightly higher accuracies in lobule V. However, none of the differences between the conditions was significant [for all regions, $t(6) < 1.704$, $P > 0.139$]. Thus the strength of the systematic modulation of different neural patches, as assessed by the classification accuracy, was roughly matched across the motor and stimulation conditions.

Table 1. *Cerebellar regions showing significant classification accuracy across participants*

Side	Area	Size, cm^3	$P_{(cluster)}$	Peak $t(6)$	SUIT		
					x	y	z
			Motor condition				
Right	Lobule V	0.84	0.001	5.94	16	−54	−24
Right	Lobule VIII	0.4	0.036	8.46	10	−70	−40
			Stimulation condition				
Right	Lobule V	0.53	0.008	6.29	22	−54	−26
Right	Lobule VIII	0.38	0.042	7.04	28	−44	−50
Right	Crus I	0.41	0.029	10.56	40	−50	−38

Random-effects analysis of classification accuracy in motor and stimulation conditions. Clusters are identified at an uncorrected threshold of $P < 0.004$, $t(6) > 3.89$, and corrected for multiple comparisons over the volume of the cerebellum using the cluster size (Worsley et al. 1996). The coordinates x, y, and z reflect the location of the peak of the cluster in SUIT space (Diedrichsen 2006).

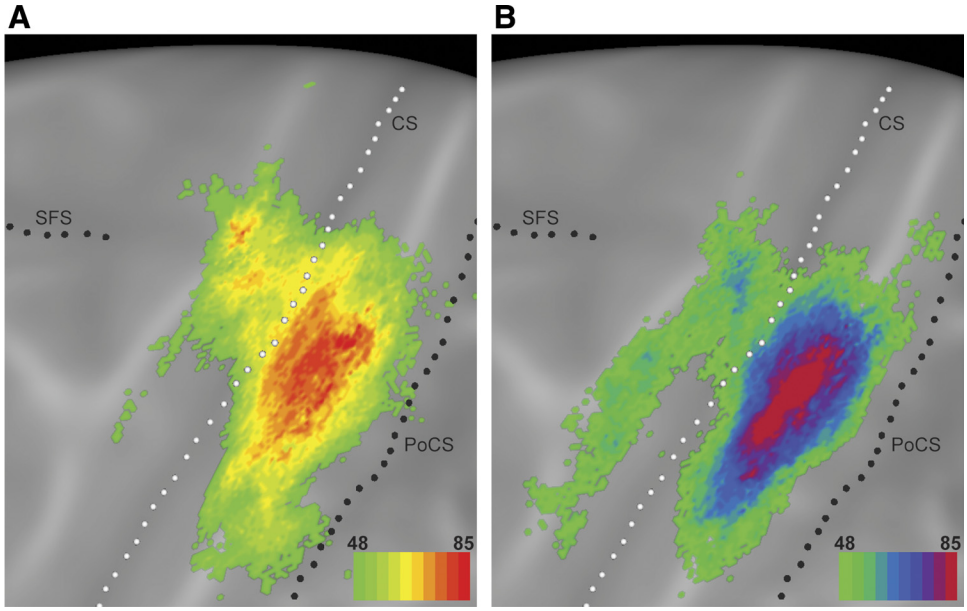

Fig. 3. Digit representation in primary motor (M1) and somatosensory cortex (S1) revealed by local multivariate pattern analysis. The group-average maps show the cross-validated classification accuracy on an inflated cortical surface for motor (*A*) and stimulation (*B*) conditions. Accuracy is shown at a 48% threshold. CS, central sulcus; PoCS, postcentral sulcus; SFS, superior frontal sulcus.

In contrast, the overall task-related activity (averaged over all digits and compared with rest, Fig. 2*B*) differed substantially between conditions. In the motor condition, we found strong activity increases in right hemispheric lobule V and VIII, bilaterally in hemispheric lobule VI, and in the vermal regions of lobule VI and VII. For sensory stimulation, however, we observed no significant evoked activity in the cerebellum. Even when we lowered the threshold to an uncorrected level of $P < 0.01$, we saw no clusters above the size of 0.13 cm^3 (corresponding to a cluster-size P value of 0.997, corrected for multiple comparison across the cerebellum).

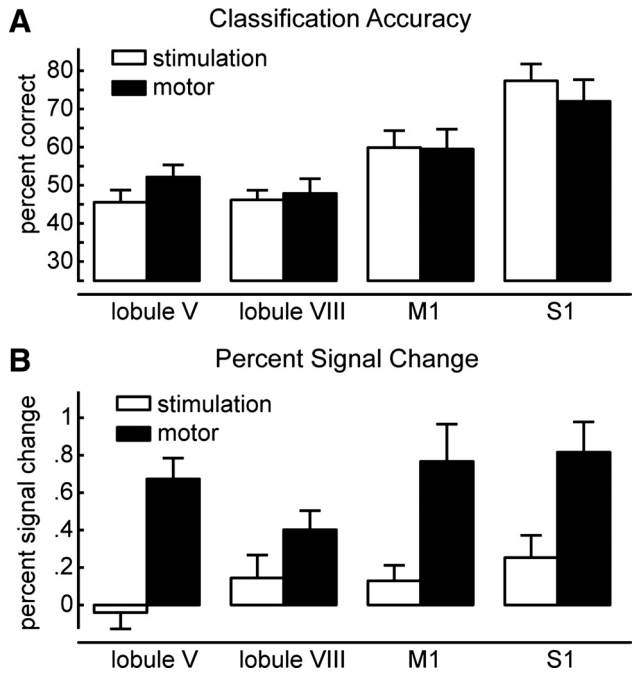

Fig. 4. Dissociation of information content and evoked activity. The digit regions were identified as the voxels with the 20% highest classification accuracies within the anatomically defined regions of interests. *A*: average classification accuracy for stimulation and motor conditions. *B*: average percent signal change (compared with rest) in the same regions. Error bars indicate between-participant standard error.

To further quantify this observation, we extracted the average percent signal change in the digit representations, which were defined as before (Fig. 4*B*). Isometric finger presses led to robust signal changes in all regions [all $t(6) > 3.86$, $P < 0.002$], whereas sensory stimulation did not [all $t(6) < 2.11$, $P > 0.078$]. In the informative region of lobule V, sensory stimulation even led on average to slight signal decreases compared with rest. This finding is consistent with previous imaging studies, which found no significant or only small signal increases during light tactile stimulation (Fox et al. 1985; Tempel and Perlmutter 1992).

Our results show that the degree to which a region increases its activity overall and the degree to which it modulates the local activity pattern based on the digit involved are partly dissociated. In the motor condition, regions with highly informative patterns also show high overall activity (Fig. 1*A*, *left*). In the stimulation condition, the informative regions did not show large increases in overall BOLD signal during task performance compared with rest. Despite this, the region showed strong finger-specific modulation. Thus we conclude that this modulation consisted of both finger-specific increases and decreases, which canceled each other out when averaged across digits (Fig. 1*A*, *right*).

Integration of sensory and motor information. Our group analysis (Fig. 2) indicates that the areas that represent force production and stimulation of single digits overlap macroscopically in the same areas, both the neocortex and the cerebellar cortex. But how is sensory and motor information integrated in these regions? Specifically, how do activation patterns caused by exerting force and stimulation superimpose? For example, it is possible that the patches of neurons that respond to stimulation of a certain finger also respond to the isometric presses with the same finger. Alternatively, force production and stimulation may activate separate patches that are independently arranged. In such an organization, a patch that is activated by a ring finger press would not necessarily be paired with a patch that is activated by ring finger stimulation but might be located right next to a patch that is activated by stimulation of the

thumb. The use of multivariate analysis allows us to distinguish between these two alternatives.

To assess the similarity between the patterns evoked by force production and stimulation, we correlated the activation patterns of two conditions across different voxels (Kriegeskorte et al. 2008a). To restrict our analysis to the region that was informative for both motor and stimulation conditions, we tested for differences between the fingers and averaged the resultant F values across motor and stimulation conditions. We then picked 20% of the voxels with the highest values. If motor and sensory representations of individual digits were mapped on top of each other, the correlation between stimulation and motor patterns from the same digit should be higher than the correlation between patterns of different digits. If the maps were organized in an independent fashion, no difference in correlation should be present.

Our results show a clearly significant difference between same-finger and different-finger correlations (Fig. 5*A*) for S1 [$t(6) = 5.18$, $P = 0.0002$] and M1 [$t(6) = 4.16$, $P = 0.006$] but no significant difference for lobule V [$t(6) = 1.90$, $P = 0.11$] and only a small difference for lobule VIII [$t(6) = 2.94$, $P = 0.026$]. Although these results may suggest weaker correlations between sensory and motor maps in the cerebellum than in the neocortex, we cannot simply compare correlations, or differences between correlations, across different regions. This is because factors other than the similarity of sensory and motor representations influence these coefficients. For example, if the fMRI data were noisier in one region, or if there were fewer informative voxels in that region, correlations, and difference in correlations, would be lower. To account for these effects, we decomposed the observed patterns into different components, each of which has characteristic variance (or power) across voxels (Diedrichsen et al. 2011). After accounting for components of no interest, we could then directly compare the correlation between the finger-specific components for stimulation and motor conditions.

Our decomposition method indeed showed that the estimated variance of the noise component was 2.5 times higher in the cerebellum than in the neocortex (Fig. 5*B*). This effect likely reflects the larger exposure to physiological noise and lower sensitivity of the coil array for subtentorial regions. In contrast, the variances of the patterns encoding specific fingers were roughly equivalent across regions (Fig. 5*C*).

Having accounted for these effects, we could now directly compare the similarity of motor and stimulation patterns for the same finger across regions (Fig. 5*D*). In the neocortex, the corrected correlation coefficient ranged between 0.12 and 0.70. In contrast, the corresponding correlations for the two cerebellar regions were significantly smaller than in the neocortex [$t(6) = -4.259$, $P = 0.005$]. Thus this analysis confirms our initial finding with uncorrected correlations was not simply due to increased noise level: In neocortical regions, stimulation and motor conditions must have activated patches of neurons that overlap in a finger-specific fashion. In contrast, in the cerebellum, patches that were activated in the motor and stimulation conditions for one particular finger must have neighbored patches that were activated by the stimulation of a different, unrelated finger. These results indicate a fundamental difference in how sensory and motor events are integrated in cerebellar and neocortical digit areas.

Size of finger patches. How large are these putative finger patches in the human cerebellum? Although the size of digit patches in S1 can be visually estimated to be between 4 and 6 mm (Nelson and Chen 2008; Sanchez-Panchuelo et al. 2010), the spatial extent of such patches cannot be assessed easily in the more irregular representations in the cerebellum or M1. One way to quantify the spatial size of digit representations is to calculate the correlation between finger-specific activations (see METHODS) for each pair of voxels within an informative region. These correlations can then be plotted as a function of the spatial distance between the voxel pair. If stimulation of each finger activates larger spatially contiguous groups of voxels, the finger effects should be correlated over longer spatial distances (Fig. 6*A*). In contrast, if the patches representing each digit are small (Fig. 6*B*), the spatial correlations should fall rapidly to zero as spatial distance increases. Indeed,

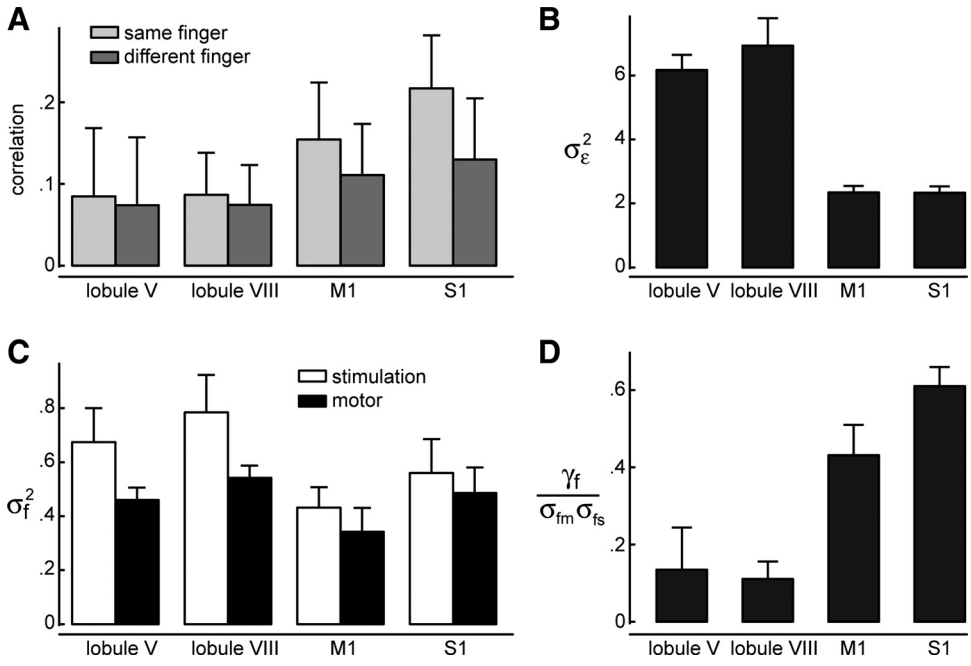

Fig. 5. Representational similarity analysis indicates different arrangement of sensory and motor maps in cortex and cerebellum. *A*: correlations between average stimulation and motor patterns for the same finger or for different fingers, calculated in digit regions of cerebellar lobule V and VIII, M1, and S1. *B*: results from variance decomposition of the correlations in *A*. Trial-by-trial noise (σ_ε^2) is increased in the cerebellum compared with neocortical regions. *C*: the variance of the patterns associated with individual fingers (σ_f^2) for stimulation and motor conditions. *D*: the normalized correlation between motor and stimulation patterns of the same digit, $\gamma_f/(\sigma_{fm}\sigma_{fs})$, is significantly reduced in cerebellar regions.

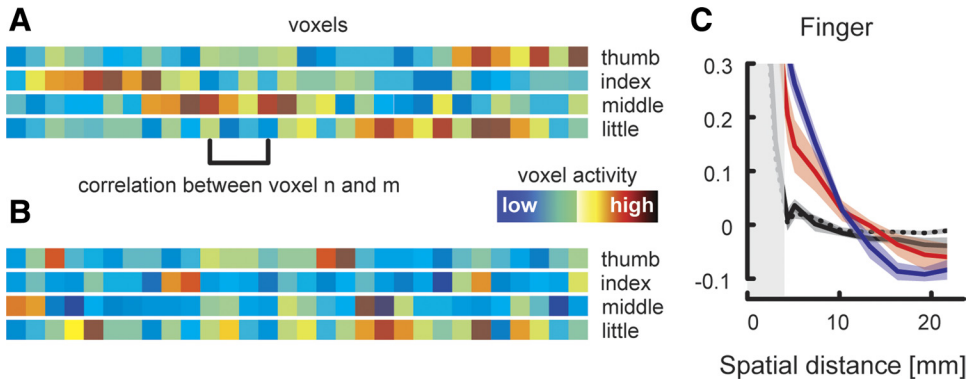

Fig. 6. Spatial correlation analysis reveals different sizes of digit patches in the neocortex compared with the cerebellum. *A*: hypothetical voxel activity related to individual fingers. If a finger activates a large patch of voxels, the correlation between voxel pairs will be positive up to a distance that relates to the size of the digit patch. *B*: if fingers activate small and scattered patches, the correlation will be absent for larger spatial distances. *C*: correlation of voxel pairs within an informative region as a function of the spatial distance of the pair. Correlations were calculated separately for the estimates for the finger component. No significant differences between motor and stimulation conditions were found; therefore, the presented data are averaged across conditions. Shaded areas indicate between-participant standard error. The vertical gray bands demark the distances for neighboring voxels, for which correlations are induced by motion correction and resampling of the images.

one can estimate the smoothness of the underlying maps (in terms of FWHM) from these spatial correlation functions (Diedrichsen et al. 2011).

The spatial correlations functions for the finger pattern component (Fig. 6*C*) revealed that in cortical regions, finger information was correlated over larger spatial distances than in the cerebellum. The FWHM of the spatial kernel in S1 was estimated to be 5 mm, and in M1, 4.1 mm, a small but significant difference [$t(6) = 2.97$, $P < 0.05$]. This result was specific to the finger effect and not found in the noise of condition effect component (Diedrichsen et al. 2011). In contrast, the finger information in cerebellar voxels was essentially uncorrelated [FWHM = 2.6 mm, significantly different from cortical regions; $t(6)=7.04$, $P < 0.05$]. We only found positive correlations for distances up to 3 mm (indicating neighboring voxels). These correlations, however, can be accounted for by head movements and the necessary spatial realignment, which induces a statistical dependence between the data of neighboring voxels (Grootoonk et al. 2000). Thus we must conclude that representations of single digits in the cerebellum are smaller than our effective resolution of 3 mm.

Somatotopy of finger representations. Thus far, our results indicate that digit patches in the cerebellum are small and arranged such that motor and sensory representations correlate with each other much less than in the neocortex. However, this independent arrangement does not preclude the existence of a systematical somatotopic gradient. Even in M1, where digit movements are represented in a highly overlapping and interdigitated fashion (Rathelot and Strick 2006; Schieber 2002), systematic differences in the centroids of activation for different digits movements have been found (Indovina and Sanes 2001; Schieber and Hibbard 1993).

To test whether there is also a somatotopic gradient for single digits in the human cerebellum, we determined for each participant and condition the CoG of the activation caused by each of the four tested digits (see METHODS). When these CoGs were displayed for lobules V in a common atlas space (Fig. 7*A*), no clear spatial organization could be seen. The center of the informative region (as indicated by spatial average location of the digit CoGs for each participant) varied substantially in mediolateral direction between individuals (Fig. 7*B*). When the CoGs for each subject were aligned by subtracting out this overall center, however, a topography became apparent (Fig. 7*C*), with the CoG for D1 being located more medially and that for D5 more laterally.

To test this observation statistically, we used a repeated-measures MANOVA on the x, y, and z coordinates of the CoGs. For the motor condition in lobule V, there was a systematic difference in the location of the finger CoGs (see Table 2). This result provides the strongest evidence to date for a somatotopic gradient in the digit representations in the cerebellum. Grodd et al.(2001) already reported a similar ordering for lobule V; however, these observations were based on a group map and were not statistically substantiated. No systematic gradient could be found in lobule VIII.

We then compared the somatotopic gradient in lobule V with those found in neocortical regions, using the effect size (η^2) of the MANOVA as a rough measure of the strength of the gradient (Table 2). The strongest gradient was detected in S1, with D1 being represented most ventrally and D5 represented most dorsally (Nelson and Chen 2008; Sanchez-Panchuelo et al. 2010). In comparison, the gradient found in lobule V was substantially weaker and more similar in strength to the one found in M1 (Fig. 7*D*), where a lateral to-medial D1–D5 gradient could be detected (see also Indovina and Sanes 2001). Overall, our results argue for a weak somatotopic organization of finger representations in the anterior, but not in the posterior, hand region of the human cerebellum.

DISCUSSION

Our results establish the existence of two overlapping representations for active force production and passive sensory stimulation of single digits in the human cerebellum. One of these is located in the ipsilateral hemisphere of lobule V and the other one in lobule VIII. In the capuchin monkey (*Cebus paella*), both of these regions have been shown to receive input from, and provide output to, the hand area of primary motor cortex (Kelly and Strick 2003).

The identification of digit representations that are close to the spatial resolution of fMRI and that do not show a systematic spatial arrangement across individuals was made possible

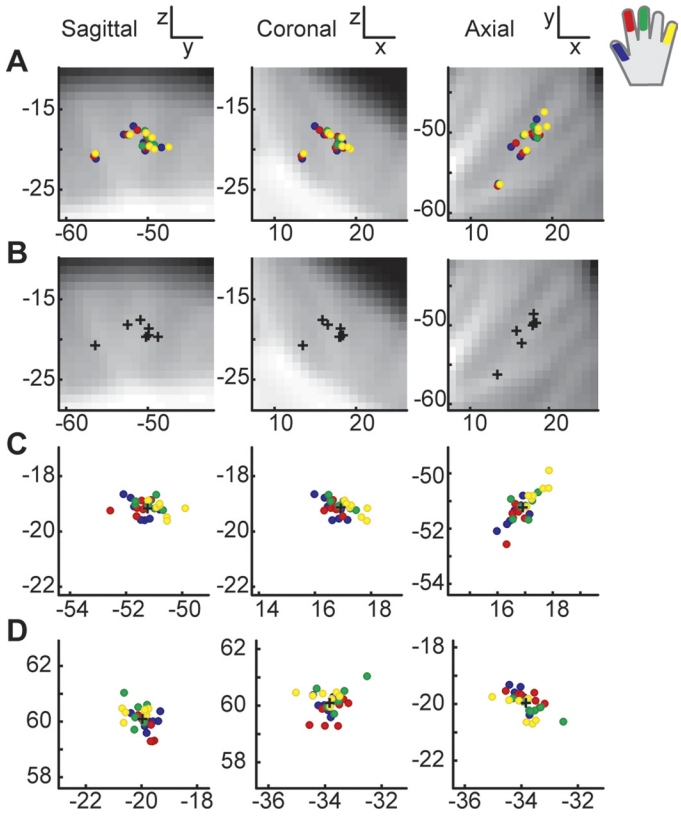

Fig. 7. Somatotopic gradient in the finger representation in lobule V and M1 for the motor condition. *A*: colored circles reflect the center of gravity (CoG) of activation elicited by force production with a single digit (D1, blue; D2, red; D3, green; and D5, yellow), presented for all participants in an average group space (SUIT). This analysis does not reveal any systematic somatotopy. *B*: the mean location of the 4 CoGs indicates the center of the informative digit region for each participant. These centers varied substantially across subjects in mediolateral direction along the folia. *C*: after the CoGs are aligned to the center of the informative region, an orderly digit representation with D1 more medial and D5 more lateral becomes apparent. *D*: aligned CoGs for fingers in the motor condition in M1. A systematic somatotopic gradient is visible with D1 represented most lateral and D5 most medial.

by employing multivariate analysis techniques (see also Kamitani and Tong 2006; Kay et al. 2008). Rather than looking for areas that increase in overall BOLD signal compared with a control condition, multivariate analysis identifies regions where the pattern of activations or deactivations differs systematically between experimental conditions. This approach is similar to that employed in many neurophysiological analyses: a neural area is considered to be involved in a task if the population of neurons encodes the factor of interest, even if on average it does not increase activity during the task.

Our results highlight the difference between information-based mapping and more traditional analysis techniques. For example, we found a number of regions that reliably increased activity in the motor condition but did not show up in the information-based analysis. One such example is the posterior vermis (lobules VI and VIII). This region has been recently shown to receive input from parts of the primary motor cortex (Coffman and Strick 2009) that relate to the proximal rather than distal musculature. Our results are consistent with this notion, because we did not detect any representation of individual digits there. Another site is lobule VI, which was consistently activated bilaterally during force production (Desmond et al. 1997; Diedrichsen et al. 2005a) but did not show evidence of single-digit representations. This region may respond preferentially to more complex movements (Schlerf et al. 2010) and may be involved in movement preparation and planning (Hulsmann et al. 2003).

For vibratory stimulation, we found regions that did not notably increase the overall BOLD-signal but modulated the activity pattern systematically with the stimulated digit. Although we found some modest increases in average activity in lobule VIII, these were far below the statistical threshold when corrected for multiple comparisons (Fox et al. 1985; Tempel and Perlmutter 1992). This finding can only be explained by the fact that vibratory stimulation led to systematic and finger-specific local increases and decreases in activation, which, when averaged over the whole area, canceled each other out (Fig. 1*A*, *right*). This is congruent with observations that vibrotactile stimulation can lead to both local increases and decreases of mossy fiber activity (Eccles et al. 1972).

One possible concern with the study is that the activity in the motor condition reflected not only motor processes but also sensory input. Although we designed our keyboard to minimize sensory feedback, Golgi-tendon organs, muscle spindle, and Merkel discs will have provided sensory information during the isometric press. Given our results, however, we think that the BOLD signal in the motor condition reflected mostly motor processes, because the overall BOLD signal was much stronger than in the sensory condition. This difference was also present in other studies that compared active to passive movement (Mima et al. 1999; Thickbroom et al. 2003). Thus, although sensory information may have contributed to our results, it is likely that active force production was the main determinant of the BOLD signal in the motor condition. Furthermore, we think that the lack of correlation between motor and sensory patterns in the cerebellum is not simply due to the fact that the two conditions activated different sensory channels: in the neocortex, sensory and motor patterns correlated highly. Although these results need to be replicated with other forms of sensory stimulation, we are relatively confident that our results reflect the interaction between motor and sensory processes.

In addition to the identification of sensory and motor digit representations, the multivariate approach allowed us to investigate the characteristics of these representations in detail. Our results suggest a fundamental difference between digit representations in human neocortex and cerebellum, with several important characteristics (summarized in Fig. 8). First, analysis

Table 2. *Statistical significance of systematic spatial ordering of finger representation in the four regions of interest*

Area	Stimulation Condition			Motor Condition		
	Λ (3, 3, 18)	P	η^2	Λ (3, 3, 18)	P	η^2
Sensory cortex	0.39	**0.059**	0.61	0.13	**>0.001**	0.87
Motor cortex	0.66	0.598	0.34	0.29	**0.011**	0.71
Lobule V	0.42	0.089	0.58	0.22	**0.002**	0.78
Lobule VIII	0.76	0.855	0.24	0.66	0.621	0.34

The first column reports Wilks Λ as a statistical test for whether there is a systematic difference in the spatial x, y, z location of the centers of gravity for the 4 fingers. P values are derived from a standard χ^2 approximation (Pearson and Hartley 1976). Effect size η^2 indicates the percent variance explained (after subtraction of the between-participant factor).

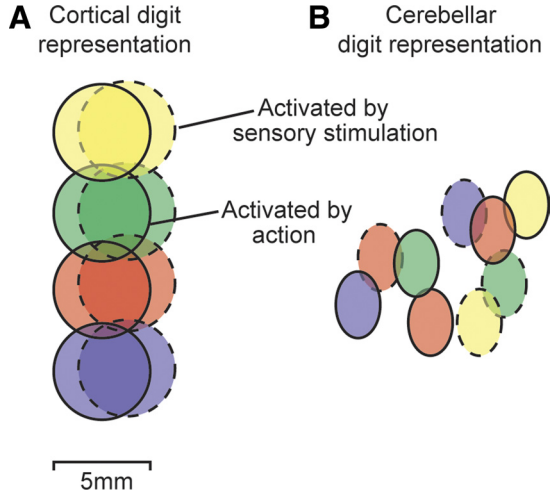

Fig. 8. Hypothetical structure of cortical and cerebellar digit representations based on the results of the multivariate analysis. *A*: in the neocortex, representations for the thumb (blue), index (red), middle (green), and little finger (yellow) are arranged in 5-mm (S1) or 4-mm (M1) large patches. The ring finger was not tested in the experiment. Patches activated by an action (solid outline) or passive vibratory stimulation (dashed outline) overlap spatially. The orderly somatotopic organization of S1 is shown, whereas the somatotopy in M1 is much less pronounced. *B*: in the cerebellum, patches are smaller than 3 mm. Sensory and motor patches for the same finger do not overlap systematically but are interdigitated in a nearly unrelated fashion.

of the spatial correlation of finger effects shows that the size of digit patches in S1 is around 5 mm and slightly smaller in M1. These numbers agree with results from monkey neurophysiology (Kaas et al. 1979; Sur et al. 1982) and human fMRI studies (Nelson and Chen 2008; Sanchez-Panchuelo et al. 2010). In the cerebellum, we found that the patterns that encoded finger information were practically uncorrelated across voxels. This argues that these representations exist at a spatial scale below the effective spatial resolution of our fMRI data (taking into account motion realignment, ~3 mm). This result is consistent with neurophysiological studies that have shown that sensory representations in the cerebellum are small and possibly fractured (Apps and Garwicz 2005; Bower and Woolston 1983). Although we cannot exclude the possibility that the difference to the neocortex was partly caused by the more complex folding structure of the cerebellum, this idea would have predicted that the spatial correlations would be higher in the direction of the folia (roughly horizontal in lobule V) than across this direction. No such spatial dependence was found, however.

Second, we showed a somatotopic gradient in lobule V of the cerebellum, where the digit representations were arranged in a medial-to-lateral order. This gradient was only significant in the motor condition and was not present in lobule VIII. Our findings are in accord with an earlier fMRI study that used a traditional group analysis (Grodd et al. 2001). At first, the presence of a somatotopic gradient may seem at odds with the small and fractured representation highlighted in our other analyses. The presence of a gradient, however, does not imply that individual digits are represented in separate patches of neurons with a strict somatotopic ordering. We found a gradient of similar strength in M1, where digit movement leads to activity in strongly overlapping population of neurons (Schieber 2002; Schieber and Hibbard 1993). Thus a weak somatotopic gradient can indeed occur within a region without a strict ordering of clearly delineated digit patches.

Third, our results show that the representations involved during passive sensory stimulation and during active force production are differently arranged in the cerebellum and the neocortex, although they overlap in both areas on a macroscopic scale. In the neocortex, we found that the pattern elicited by pressing a particular finger was similar to the pattern elicited by sensory stimulation of the same finger. This indicates that patches that are activated by sensory stimulation are also active during isometric contraction of the same finger (Fig. 8*A*). In contrast, this correlation was significantly smaller in the cerebellum. We are confident that this finding was not an artifact of the increased noise or the smaller size of the representations; we employed a new variance decomposition technique that can be shown to be able to estimate the representational overlap independently of these factors (Diedrichsen et al. 2011).

What underlying neurobiological architectures might give rise to such a finding? One possibility is that sensory and motor processes activate separate sets of neuronal maps. However, given that the cerebellum is often considered to be a site where sensory and motor information are integrated (Gao et al. 1996; Wolpert et al. 1998), such architecture would be surprising. Furthermore, in our group analysis, the informative regions for motor and stimulation condition overlapped substantially, and no significant difference in mean location was found. We suggest that our results are congruent with the following arrangement (Fig. 8*B*): cerebellar digit patches that modulate their responses during active motor output and during passive stimulation may be closely interdigitated. However, patches that are activated by action of a particular digit directly neighbor, or even overlap with, patches that are activated by sensory stimulation of a different digit. Thus sensory and motor patches referring to the same finger would not overlap with much higher probability than sensory and motor patches of unrelated fingers. Such an organization would account for the finding of macroscopic spatial overlap but low correlation between patterns.

What could the computational function of such an arrangement be? In the neocortex, the movement of each digit is closely paired with the most likely sensory consequence of that action, sensory stimulation of the same finger. In contrast, in the cerebellum, movement of a digit may lead to activity in neurons that are also activated by a variety of different sensory consequences, ranging from stimulation of other fingers to maybe even sensory input from the arm or face. Such an arrangement may enable the cerebellum to quickly form new associations between movements and relatively arbitrary, remote sensory consequences. This is a key computational requirement for learning new motor tasks, in which actions and outcomes can take on novel and never before experienced relationships. Consistent with this functional hypothesis, cerebellar patients are severely and specifically impaired on such tasks (Diedrichsen et al. 2005b; Smith and Shadmehr 2005). In summary, the way motor and sensory events are represented may support the quick learning of action-outcome associations (i.e., forward models), which has been hypothesized to be the main computational function of the cerebellum (Wolpert et al. 1998).

ACKNOWLEDGMENTS

We thank Nikolaas Oosterhof for helpful discussions on multivariate and surface-based analysis.

GRANTS

This work was supported by National Science Foundation Grant BSC 0726685 (to J. Diedrichsen) and Welsh Institute of Cognitive Neuroscience Grant WBC027 (to D. MJ. McGonigle and J. Diedrichsen).

DISCLOSURES

No conflicts of interest, financial or otherwise, are declared by the author(s).

REFERENCES

Apps R, Garwicz M. Anatomical and physiological foundations of cerebellar information processing. *Nat Rev Neurosci* 6: 297–311, 2005.

Ashburner J, Friston KJ. Unified segmentation. *Neuroimage* 26: 839–851, 2005.

Attwell D, Iadecola C. The neural basis of functional brain imaging signals. *Trends Neurosci* 25: 621–625, 2002.

Bastian AJ. Learning to predict the future: the cerebellum adapts feedforward movement control. *Curr Opin Neurobiol* 16: 645–649, 2006.

Bower JM, Woolston DC. Congruence of spatial organization of tactile projections to granule cell and Purkinje cell layers of cerebellar hemispheres of the albino rat: vertical organization of cerebellar cortex. *J Neurophysiol* 49: 745–766, 1983.

Casey KL, Minoshima S, Morrow TJ, Koeppe RA. Comparison of human cerebral activation pattern during cutaneous warmth, heat pain, and deep cold pain. *J Neurophysiol* 76: 571–581, 1996.

Coffman KA, Strick PL. The primary motor cortex is a source of input to the posterior vermis. *Soc Neurosci Abstr* 367.326, 2009.

Collignon A, Maes F, Delaere D, Vandermeulen D, Suetens P, Marchal G. Automated multi-modality image registration based on information theory. In: *14th International Conference*, edited by Bizais Y, Barillot C, Di Paola R. Ile de Berder, France: Springer, 1995, p. 263–274.

Cox DD, Savoy RL. Functional magnetic resonance imaging (fMRI) "brain reading": detecting and classifying distributed patterns of fMRI activity in human visual cortex. *Neuroimage* 19: 261–270, 2003.

Dale AM, Fischl B, Sereno MI. Cortical surface-based analysis. I. Segmentation and surface reconstruction. *Neuroimage* 9: 179–194, 1999.

Desmond JE, Gabrieli JD, Wagner AD, Ginier BL, Glover GH. Lobular patterns of cerebellar activation in verbal working-memory and finger-tapping tasks as revealed by functional MRI. *J Neurosci* 17: 9675–9685, 1997.

Diedrichsen J. A spatially unbiased atlas template of the human cerebellum. *Neuroimage* 33: 127–138, 2006.

Diedrichsen J, Balsters JH, Flavell J, Cussans E, Ramnani N. A probabilistic MR atlas of the human cerebellum. *Neuroimage* 46: 39–46, 2009.

Diedrichsen J, Hashambhoy Y, Rane T, Shadmehr R. Neural correlates of reach errors. *J Neurosci* 25: 9919–9931, 2005a.

Diedrichsen J, Ridgway GR, Friston KJ, Wiestler T. Comparing the similarity and spatial structure of neural representations: a pattern-component model. *Neuroimage* 55: 1665–1678, 2011.

Diedrichsen J, Verstynen T, Lehman SL, Ivry RB. Cerebellar involvement in anticipating the consequences of self-produced actions during bimanual movements. *J Neurophysiol* 93: 801–812, 2005b.

Diedrichsen J, Verstynen T, Schlerf J, Wiestler T. Advances in functional imaging of the human cerebellum. *Curr Opin Neurol* 23: 382–387, 2010.

Eccles JC, Sabah NH, Schmidt RF, Taborikova H. Cutaneous mechanoreceptors influencing impulse discharges in cerebellar cortex. I. In mossy fibers. *Exp Brain Res* 15: 245–260, 1972.

Fox PT, Raichle ME, Thach WT. Functional mapping of the human cerebellum with positron emission tomography. *Proc Natl Acad Sci USA* 82: 7462–7466, 1985.

Friston KJ, Worsley KJ, Frackowiak RSJ, Mazziotta JC, Evans AC. Assessing the significance of focal activations using their spatial extent. *Hum Brain Mapp* 1: 210–220, 1993.

Gao JH, Parsons LM, Bower JM, Xiong J, Li J, Fox PT. Cerebellum implicated in sensory acquisition and discrimination rather than motor control. *Science* 272: 545–547, 1996.

Geyer S, Schleicher A, Schormann T, Mohlberg H, Bodegard A, Roland PE, Zilles K. Integration of microstructural and functional aspects of human somatosensory areas 3a, 3b, and 1 on the basis of a computerized brain atlas. *Anat Embryol (Berl)* 204: 351–366, 2001.

Grodd W, Hulsmann E, Lotze M, Wildgruber D, Erb M. Sensorimotor mapping of the human cerebellum: fMRI evidence of somatotopic organization. *Hum Brain Mapp* 13: 55–73, 2001.

Grootoonk S, Hutton C, Ashburner J, Howseman AM, Josephs O, Rees G, Friston KJ, Turner R. Characterization and correction of interpolation effects in the realignment of fMRI time series. *Neuroimage* 11: 49–57, 2000.

Haxby JV, Gobbini MI, Furey ML, Ishai A, Schouten JL, Pietrini P. Distributed and overlapping representations of faces and objects in ventral temporal cortex. *Science* 293: 2425–2430, 2001.

Haynes JD, Rees G. Predicting the orientation of invisible stimuli from activity in human primary visual cortex. *Nat Neurosci* 8: 686–691, 2005a.

Haynes JD, Rees G. Predicting the stream of consciousness from activity in human visual cortex. *Curr Biol* 15: 1301–1307, 2005b.

Hulsmann E, Erb M, Grodd W. From will to action: sequential cerebellar contributions to voluntary movement. *Neuroimage* 20: 1485–1492, 2003.

Indovina I, Sanes JN. On somatotopic representation centers for finger movements in human primary motor cortex and supplementary motor area. *Neuroimage* 13: 1027–1034, 2001.

Johnson KO. The roles and functions of cutaneous mechanoreceptors. *Curr Opin Neurobiol* 11: 455–461, 2001.

Kaas JH, Nelson RJ, Sur M, Lin CS, Merzenich MM. Multiple representations of the body within the primary somatosensory cortex of primates. *Science* 204: 521–523, 1979.

Kamitani Y, Tong F. Decoding seen and attended motion directions from activity in the human visual cortex. *Curr Biol* 16: 1096–1102, 2006.

Kay KN, Naselaris T, Prenger RJ, Gallant JL. Identifying natural images from human brain activity. *Nature* 452: 352–355, 2008.

Kelly RM, Strick PL. Cerebellar loops with motor cortex and prefrontal cortex of a nonhuman primate. *J Neurosci* 23: 8432–8444, 2003.

Kriegeskorte N, Goebel R, Bandettini P. Information-based functional brain mapping. *Proc Natl Acad Sci USA* 103: 3863–3868, 2006.

Kriegeskorte N, Mur M, Bandettini P. Representational similarity analysis—connecting the branches of systems neuroscience. *Front Syst Neurosci* 2: 4, 2008a.

Kriegeskorte N, Mur M, Ruff DA, Kiani R, Bodurka J, Esteky H, Tanaka K, Bandettini PA. Matching categorical object representations in inferior temporal cortex of man and monkey. *Neuron* 60: 1126–1141, 2008b.

Merzenich MM, Nelson RJ, Kaas JH, Stryker MP, Jenkins WM, Zook JM, Cynader MS, Schoppmann A. Variability in hand surface representations in areas 3b and 1 in adult owl and squirrel monkeys. *J Comp Neurol* 258: 281–296, 1987.

Mima T, Sadato N, Yazawa S, Hanakawa T, Fukuyama H, Yonekura Y, Shibasaki H. Brain structures related to active and passive finger movements in man. *Brain* 122: 1989–1997, 1999.

Misaki M, Kim Y, Bandettini PA, Kriegeskorte N. Comparison of multivariate classifiers and response normalizations for pattern-information fMRI. *Neuroimage* 53: 103–118, 2010.

Mur M, Bandettini PA, Kriegeskorte N. Revealing representational content with pattern-information fMRI—an introductory guide. *Soc Cogn Affect Neurosci* 4: 101–109, 2009.

Nelson AJ, Chen R. Digit somatotopy within cortical areas of the postcentral gyrus in humans. *Cereb Cortex* 18: 2341–2351, 2008.

Norman KA, Polyn SM, Detre GJ, Haxby JV. Beyond mind-reading: multi-voxel pattern analysis of fMRI data. *Trends Cogn Sci* 10: 424–430, 2006.

Oosterhof NN, Wiestler T, Downing PE, Diedrichsen J. A comparison of volume-based and surface-based multi-voxel pattern analysis. *Neuroimage*. In press.

Pearson ES, Hartley HO. *Biometrika Tables for Statisticians*. Cambridge, UK: Cambridge University Press, 1976.

Pereira F, Mitchell T, Botvinick M. Machine learning classifiers and fMRI: a tutorial overview. *Neuroimage* 45: S199–S209, 2009.

Peyre G. Toolbox Fast Marching—A toolbox for Fast Marching and level sets computations (Online). http://www.ceremade.dauphine.fr/~peyre/matlab/fast-marching/content.html.

Pruessmann KP, Weiger M, Scheidegger MB, Boesiger P. SENSE: sensitivity encoding for fast MRI. *Magn Reson Med* 42: 952–962, 1999.

Rathelot JA, Strick PL. Muscle representation in the macaque motor cortex: an anatomical perspective. *Proc Natl Acad Sci USA* 103: 8257–8262, 2006.

Rijntjes M, Buechel C, Kiebel S, Weiller C. Multiple somatotopic representations in the human cerebellum. *Neuroreport* 10: 3653–3658, 1999.

Sanchez-Panchuelo RM, Francis S, Bowtell R, Schluppeck D. Mapping human somatosensory cortex in individual subjects with 7T functional MRI. *J Neurophysiol* 103: 2544–2556, 2010.

Schieber MH. Motor cortex and the distributed anatomy of finger movements. *Adv Exp Med Biol* 508: 411–416, 2002.

Schieber MH, Hibbard LS. How somatotopic is the motor cortex hand area? *Science* 261: 489–492, 1993.

Schlerf JE, Verstynen TD, Ivry RB, Spencer RM. Evidence of a novel somatopic map in the human neocerebellum during complex actions. *J Neurophysiol* 103: 3330–3336, 2010.

Smith MA, Shadmehr R. Intact ability to learn internal models of arm dynamics in Huntington's disease but not cerebellar degeneration. *J Neurophysiol* 93: 2809–2821, 2005.

Sur M, Nelson RJ, Kaas JH. Representations of the body surface in cortical areas 3b and 1 of squirrel monkeys: comparisons with other primates. *J Comp Neurol* 211: 177–192, 1982.

Swisher JD, Gatenby JC, Gore JC, Wolfe BA, Moon CH, Kim SG, Tong F. Multiscale pattern analysis of orientation-selective activity in the primary visual cortex. *J Neurosci* 30: 325–330, 2010.

Tempel LW, Perlmutter JS. Vibration-induced regional cerebral blood flow responses in normal aging. *J Cereb Blood Flow Metab* 12: 554–561, 1992.

Thickbroom GW, Byrnes ML, Mastaglia FL. Dual representation of the hand in the cerebellum: activation with voluntary and passive finger movement. *Neuroimage* 18: 670–674, 2003.

Wolpert DM, Miall RC, Kawato M. Internal models in the cerebellum. *Trends Cogn Sci* 2: 313–321, 1998.

Woolsey CN, Erickson TC, Gilson WE. Localization in somatic sensory and motor areas of human cerebral cortex as determined by direct recording of evoked potentials and electrical stimulation. *J Neurosurg* 51: 476–506, 1979.

Worsley KJ, Marrett S, Neelin P, Vandal AC, Friston KJ, Evans AC. A unified statistical approach for determining significant voxels in images of cerebral activation. *Hum Brain Mapp* 12: 900–918, 1996.

Yousry TA, Schmid UD, Alkadhi H, Schmidt D, Peraud A, Buettner A, Winkler P. Localization of the motor hand area to a knob on the precentral gyrus. A new landmark. *Brain* 120: 141–157, 1997.

Zhang Y, Forster C, Milner TA, Iadecola C. Attenuation of activity-induced increases in cerebellar blood flow by lesion of the inferior olive. *Am J Physiol Heart Circ Physiol* 285: H1177–H1182, 2003.